

Mechanical determination of internal stresses in as-quenched magnetic amorphous metallic ribbons

M. TEJEDOR, J. A. GARCÍA, J. CARRIZO, L. ELBAILE

Universidad de Oviedo, Departamento de Física, Calvo Sotelo S/N, 33007 Oviedo, Spain

The layer removing method for determining the internal stress distribution through thickness in sheets has been applied to metallic glass ribbons. The internal stresses are obtained from the variation of the radius of curvature of the samples when the layers are removed. The experimental technique used is described here and the results for two ribbons, are presented. A general feature has been observed implying compressive stress near both surfaces (a strong one near the drum surface and a weak one near the air surface), and the central part under tensile stress. This is in agreement with the residual stress distribution shown by other materials after fast cooling procedures.

1. Introduction

Metallic glasses are widely applied for different commercial applications. Besides their classical use in power devices (inverter transformers and motors), in recent years they are being increasingly used in various other fields of electronics, as in magnetic heads, magnetic sensors and transducers. The growth of such applications is due to their good magnetic, mechanical, magnetoelastic, electrical properties and easy obtention. Other reason that explains the wide range of their applications is the fact that their magnetic and structural properties can be controlled and varied by alloy composition and subsequent thermomagnetic treatments. They also have other advantages which are not shown by the conventional crystalline soft magnetic materials such as their high electrical resistivity, production-inherent low thickness and favourable surface properties.

In magnetostrictive metallic glasses the magnetoelastic coupling factor (K) has values slightly under 1 and the variation of Young's modulus with the magnetic field (ΔY) reaches huge values (above 100%). These two properties show that metallic glasses are excellent for applications based in magnetoelastic effects.

These amorphous magnetic materials are excellent soft magnetic materials because they do not present magnetocrystalline anisotropy and structural defects. Nevertheless, owing to the manufacture process, they show magnetic anisotropy that impairs their above-mentioned good soft magnetic properties. One of the different causes generating the magnetic anisotropy is the presence of residual stresses which may exist in the material free of external load.

The majority of metallic glasses are prepared by quenching a molten stream of an alloy onto the surface of a spinning drum. This method originates a

temperature difference between surface and core that generates internal stresses owing to their inherent rapid solidification (10^5 – 10^6 K s⁻¹). The properties of these materials are sensitive to mechanical strain; therefore, it is very important to assess their internal stress distribution from the point of view of general knowledge and also in order to improve their properties with a view to technical applications.

As far as we know, all the estimations about the internal stresses in these materials have been inferred from magnetic measurements, direct mechanical measurements never having been made.

Knowing the residual stress distribution in magnetic samples is crucial to explain, in some cases, the existence of magnetic anisotropy. Ok and Morrish [1] have proposed a model based in the existence of compressive stress in the bulk and tensile stress near the surfaces in annealed amorphous magnetic materials, to explain in them the existence of perpendicular magnetic anisotropy.

One of the most widely used technique to determine the internal stress is X-ray diffraction, based on the internal stresses' production of changes in the lattice parameter which are measured as shifts in the X-ray diffraction angle. However, due to the lack of internal structure shown by amorphous magnetic materials, this method is not applicable in this case. Different mechanical methods have been developed in order to study the residual stress distribution in thin-walled tubing [2], bent sheet metals [3], laser treated steels [4,5] and thin films [6]. In this paper the removal of surface layers method has been adapted to study the distribution through the thickness of the residual stresses in metallic glasses. This method has already been applied with success to study the residual stresses in sheet samples [7], and thin coatings [8].

We have applied this method to two magnetic metallic glasses with different composition and properties. The residual stress distribution thus obtained closely agrees with that obtained on an aluminium AA7075 T4 alloy plate quenched in hot and cold water [9], with the predictions about the residual stresses in cooled materials without phase transformation [10], and with the magnetoelastic perpendicular magnetic anisotropy observed by studies of the magnetic domains structure in magnetostrictive amorphous ribbons [11].

2. Stress analysis and its relationship with curvature

In this work internal stresses have been obtained from the variation of the curvature of the sample using the removal of surface layers method. For this purpose, it is necessary for the material to be linear in pure bending and the stress not to vary in the plane, but only through the thickness. In addition, the method used for removing the layers should not produce any additional stress.

A correct formulation of the bending process is required to obtain the relationship between stress and curvature. The study of metal bending was developed in the early 1950s and 1960s in different papers [12,13,14] and has extensively been applied to the spring back of metals [15].

In short, the calculations we have worked out taking into account the above mentioned papers contemplate flat samples of thickness t , Young's modulus E and Poisson's ratio ν , subject to the condition that the stress only varies through the thickness, and so it can be defined by its principal components in the plane of the sample.

Owing to the fact that internal stresses are self-equilibrating, the equilibrium conditions will be

$$\int_{-t/2}^{t/2} \sigma_x(z) dz = \int_{-t/2}^{t/2} \sigma_x(z)z dz = 0$$

$$\int_{-t/2}^{t/2} \sigma_y(z) dz = \int_{-t/2}^{t/2} \sigma_y(z)z dz = 0 \quad (1)$$

If we remove a uniform layer of the material from one of the surfaces, the equilibrium is broken and an unbalanced distribution of internal stress appears. The constraint applied by the layer disappears and the remainder of the sample will deform elastically under the action of the unbalanced internal stress until a new equilibrium is reached. A purely elastic response is supposed due to the very high elastic limit of these materials [16]. It is well known that if the sample is flat and isotropic, it bends into a spherical surface. If the internal stress, however, is mainly in one direction in the plane, the flat sample bends into a cylindrical surface (Fig. 1). In this case, the constraint applied by the removed layer on the remainder of the sample can be replaced by a force N_t and a moment M_t per unit of width, which are equal and opposite to those obtained by integrating the residual stress across the current thickness.

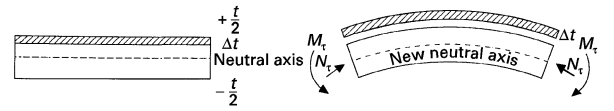


Figure 1 Bend of a plane plate after removal of a tensioned layer.

The bending moment that produces the bend of the sample would be [17]

$$M_t = \frac{E(t - \Delta t)^3}{12(1 - \nu^2)} \frac{1}{R} \quad (2)$$

where R is the radius of curvature of the cylindrical surface.

Taking into account that $M_t = N_t t - \Delta t/2$ the value of the resultant removed layer force will be [17]

$$N_t = \frac{E(t - \Delta t)^2}{6(1 - \nu^2)} \frac{1}{R} \quad (3)$$

If the removed layer is very thin, we can consider that the stress is constant across it, and its value becomes

$$\sigma_0 = \frac{E(t - \Delta t)^2}{6\Delta t(1 - \nu^2)} \frac{1}{R} \quad (4)$$

and the axial stress $\sigma_1(z)$ induced in the remainder sample by the tangential stress

$$\sigma_1(z) = \frac{N_t}{t - \Delta t} + \frac{M_t}{\frac{1}{12}(t - \Delta t)^2}$$

$$= \frac{\sigma_0 \Delta t}{t - \Delta t} \left(1 + \frac{6z}{t - \Delta t} \right) \quad (5)$$

with the neutral axis $z = 0$ in the middle of the sample less the removed layer.

The axial stress disappears when the layer is removed, taking into account its value when calculating the stress in the layers to be removed subsequently.

When a new layer of thickness $\Delta t'$ is removed from the surface, the sample will change into another cylindrical surface of radius R' , and the stress in the layer removed producing this change of curvature, becomes

$$\sigma' = \frac{E(t - \Delta t - \Delta t')^2}{6\Delta t'(1 - \nu^2)} \left(\frac{1}{R'} - \frac{1}{R} \right) \quad (6)$$

The internal stress σ_0' in the thin removed layer would be σ' plus the stress $\sigma_1(z_1)$ (Equation 5), z_1 being the distance to the centre line of the layer removed in the second turn (Fig. 2)

$$\sigma_0' = \sigma' + \sigma_1(z_1) \quad (7)$$

The tangential stress induces axial stress $\sigma_2(z)$ in the remainder of the sample in the same way as the first removed layer did, being, similarly

$$\sigma_2(z) = \frac{\sigma' \Delta t'}{(t - \Delta t - \Delta t')} \left(1 + \frac{6z}{t - \Delta t - \Delta t'} \right) \quad (8)$$

and so on, with other removed layers, the determination of the residual stress distribution throughout the whole thickness of the material being possible in this way.

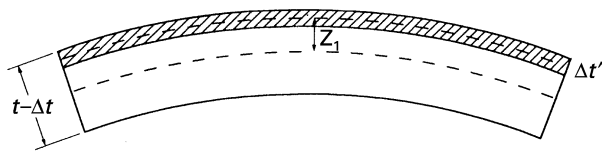


Figure 2 Cross-section showing the middle fibre of the layer z_1 to be removed in a plate.

3. Experimental Procedure

To determine the radius of curvature of the sample we used a microscope previously calibrated for a known sample. The maximum deflection h is determined from the difference between the readings, focusing at the top and at the bottom of the sample. The radius of curvature as a function of h and the cord x of the curved sample will be

$$R = \frac{x^2}{8h} + \frac{h}{2} \quad (9)$$

The sign of the stress is determined by the bend of the sample in the following way: if layers are being removed from the top to the bottom of the sample (Fig. 2), and this changes to a more convex shape, the internal stress is considered positive (tensile stress), but if it becomes more concave, internal stress is considered negative (compressive stress). If layers are removed from the bottom to the top, the results are inverted.

For the study of internal stress distribution, circular samples are desirable in order to avoid any shape effects. So in order to produce these, one can start by cutting off a quasi-circular sample from the ribbon, completing the process by mechanical polishing of the edge by fixing the sample to a lathe spindle, and bringing a grindstone up to the sample edge when turning. By this process, highly perfect discs with negligible excentricity are obtained. The amorphous magnetic materials are now available in ribbons of various centimetre dimensions, which allows the production of discs with a size sufficient to perform the necessary measurements. The discs were cut out from two different ribbons and they have the following compositions and mechanical properties: $\text{Ni}_{40}\text{Fe}_{40}(\text{Si} + \text{B})_{19}\text{Mo}_{1-2}$ with a tensile strength of 1500–2000 MPa, tensile modulus of 150 GPa and hardness (Vickers) of 7.84 MN mm^{-2} and $\text{Co}_{70}(\text{Si} + \text{B})_{23}\text{Mn}_5(\text{Fe} + \text{Mo})_2$ with a tensile strength of 1500–2000 MPa, tensile modulus of 150 GPa and hardness (Vickers) of 8.82 MN mm^{-2} . We use a value of 0.33 for the Poisson's ratio in the two cases. The mechanical properties data are obtained from the 1996 catalogue of Goodfellow (UK). The discs' diameters were 16.90 mm, 16.65 mm, 19.15 mm and 19.30 mm for the $\text{Co}_{70}(\text{Si} + \text{B})_{23}\text{Mn}_5(\text{Fe} + \text{Mo})_2$ samples and 19.65 mm, 19.00 mm, 22.75 mm, 17.55 mm, 16.70 mm and 17.00 mm for the $\text{Ni}_{40}\text{Fe}_{40}(\text{Si} + \text{B})_{19}\text{Mo}_{1-2}$ samples.

To remove the layers, electrolytic polishing was performed according to the conventional method described by Chikazumi [18]. This method does not induce any additional stress in the sample that might

alter the results. The thickness of the removed surface layer has been determined by measuring the weight of the sample before and after polishing. The profile of the samples before and after each electrolytical polishing was measured by a profilograph with a sensitivity of $0.1 \mu\text{m}$. The results obtained indicate that the profile of the samples before and after the electrolytic polishings are practically the same, indicating a uniform removal. All the samples have an initial thickness of $40 \mu\text{m}$ enough to perform a sufficient number of polishings. A set of samples was polished from one surface to the other and another set in the opposite way. The displacement of the centre of each sample relative to the edges when the bending occurs after the electrolytic polishing was of the order of tenths of millimetres, enough for an accurate measurement with the microscope.

4. Results and discussion

The amorphous ribbons in the as-quenched state show cylindrical curvature in the transverse direction with the drum surface in the convex side, indicating the internal stresses produced during the rapid quenching in the manufacturing process.

Because, in our samples, the radius is large in comparison with the plate thickness ($R/t \geq 2000$), the internal stress in the direction of the thickness can be neglected. Furthermore, the width b of the plate is rather wide if compared with its thickness ($b/t \geq 400$) and it is possible to assume the plane strain bending. The uniformity of the bending of the samples in the as-quenched state and after each electrolytic polishing was checked with a profile projector.

On removal of the surface layers, the samples show changes of the values of their cylindrical curvatures. The results obtained for the consequent stress distribution throughout the thickness are shown in Fig. 3. It can be seen that in the two materials, both surfaces of the ribbon are in compressive stress, whilst the central part of the ribbons are in tensile stress. The depth surface zones are between 5 and $10 \mu\text{m}$ on both sides. A similar behaviour was observed in other kind of materials after a quenching process [9] and it was explained for quenched materials without phase transformation by Mayr [10]; in a quenching process, the surface cools more quickly and shrinks more severely than the core in the beginning. In this phase there are tensile stresses on the surface and compressive stresses in the core, but beyond the point of highest temperature difference between the surface and the core, the core shrinks faster than the surface, which leads to a decrease of the surface stress until the point of stress conversion and after the surface falls under compression and the core under tension.

In our case, the curve representing stress versus thickness has no symmetry. This behaviour can be expected because, in these ribbons, only the drum surface is in contact with the thermal sink and it explain the above mentioned initial curvature of the samples. Other characteristic of these curves is the fact that the great compressive stress developed near the drum surface (30 MPa in $\text{Ni}_{40}\text{Fe}_{40}(\text{Si} + \text{B})_{19}\text{Mo}_{1-2}$

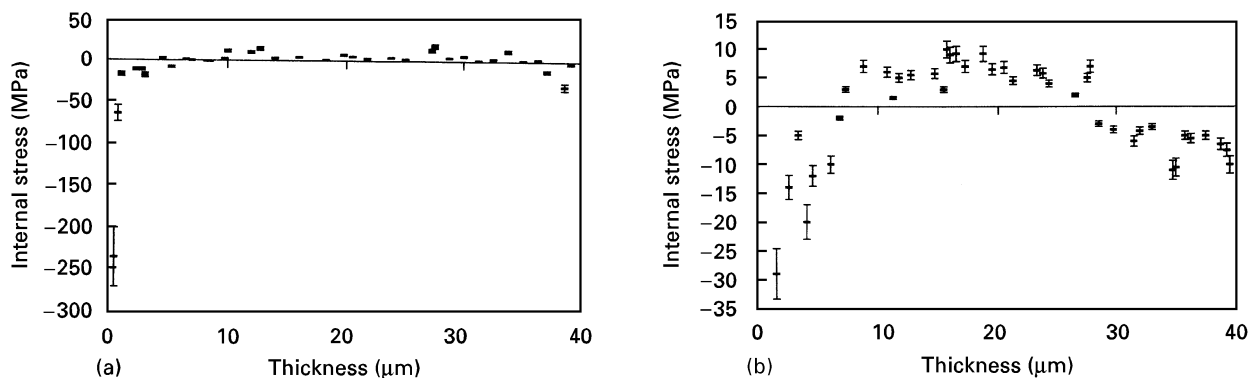


Figure 3 Internal stress distribution through the thickness of the plate in (a) $\text{Co}_{70}(\text{Si} + \text{B})_{23}\text{Mn}_5(\text{Fe} + \text{Mo})_2$ and (b) $\text{Ni}_{40}\text{Fe}_{40}(\text{Si} + \text{B})_{19}\text{Mo}_{1-2}$. Thickness zero begins in the drum-surface of the plate.

and near 250 MPa in $\text{Co}_{70}(\text{Si} + \text{B})_{23}\text{Mn}_5(\text{Fe} + \text{Mo})_2$ drops dramatically to zero in both samples.

This internal stress distribution in magnetic amorphous materials is in agreement with the observation of closure magnetic domains in drum and air surfaces made by one of the authors [12] on $\text{Fe}_{40}\text{Ni}_{40}\text{P}_{14}\text{B}_6$ amorphous ribbons. The domain patterns observed are typical of ferromagnetic materials which possess an easy anisotropy axis perpendicular to the surface near this. The magnitude of the perpendicular anisotropy determines the type of domain structure and the domain width, as discussed in Tsukahara *et al.* [19]. Applying the Chikazumi and Suzuki formula for the width of zig-zag closure domains [20], the square of the width is inversely proportional to the mean stress in the closure domains. Taking into account that the domain width in the drum surface is less than that in the air surface, it follows that the stress in the drum side is greater than that in the air side.

The volumes deduced from our measurements corresponding to tensile and compressive values of the stress are very similar. This result is in agreement with the estimation made by Vazquez *et al.* [21] from magnetic considerations.

5. Conclusions

The authors have deduced by mechanical measurements the internal stress distribution in as-quenched magnetic amorphous ribbons. Two different zones have been distinguished: (a) the region near the surfaces which is under compression stress and (b) the central part which is under tension stress, being far greater in the drum surface. The different cooling rates of the two zones during the manufacturing process is supposed to be the origin of this internal stress distribution. Such internal stress distribution agrees with perpendicular magnetic anisotropy deduced by domain structure observations in as-quenched samples with positive magnetostriction.

Acknowledgements

This work was supported in part by the CICYT under grant no. MAT 93-0440 (Madrid, Spain).

References

1. H.N. OK and A.H. MORRISH, *Phys. Rev. B* **23** (1981) 2257.
2. G. SACHS and G. SPEY, *Trans. AIME* **147** (1942) 348.
3. T. TAN, W.B. LI and B. PERSSON, *Int. J. Mech. Sci.* **36** (1994) 483.
4. R. KRÁLOVÁ, *Mater. Sci. Eng.* **A147** (1994) L51.
5. R. KRÁLOVÁ, *J. Mater. Sci. Lett.* **12** (1993) 1951.
6. E. DU TREMOLET and J.C. PEUZIN, *J. Magn. Magn. Mater.* **136** (1994) 189.
7. R.G. TREUTING and W.T. READ JR., *J. Appl. Phys.* **22** (1951) 130.
8. P.M. RAMSEY, H.W. CHANDLER and T.F. PAGE, *Surf. Coat. Technol.* **43/4** (1990) 223.
9. G. BECK, in "Residual stress in science and technology" Vol. 1, edited by E. Macherauch and V. Hauk (DGM Informationsgesellschaft, Oberusel, 1987) p. 27.
10. P. MAYR in "Residual stress in science and technology" Vol. 1, edited by E. Macherauch and V. Hauk (DGM Informationsgesellschaft, Oberusel, 1987) p. 57.
11. M. TEJEDOR and B. HERNANDO, *J. Phys. D: Appl. Phys.* **13** (1980) 1709.
12. J.D. LUBAHN and G. SACHS, *Trans. ASME* **72** (1950) 201.
13. J.M. ALEXANDER, *Proc. Inst. Mech. Eng.* **173** (1950) 73.
14. A. DENTON, *J. Strain Anal.* **3** (1996) 197.
15. O.M. SIDEBOTTOM and C.F. GEBHARDT, *Exp. Mech.* **October** (1979) 371.
16. J. GONZALEZ, V. MADURGA, M. POZA and A. HERNANDO, *J. Phys. D: Appl. Phys.* **14** (1981) 1143.
17. J.P. DEN HARTOG in "Advanced strength of materials" (Dover Publications, Inc., New York, 1987) Chapters III and IV.
18. S. CHIKAZUMI, in "Physics of magnetism" (Wiley, New York, 1964), p. 221.
19. S. TSUKAHARA, T. SATOH and T. TSUSHIMA, *IEEE Trans. Magn.* **MAG 14** (1978) 1022.
20. S. CHIKAZUMI and K. SUZUKI, *J. Phys. Soc. Jpn* **10** (1955) 523.
21. M. VAZQUEZ, A. HERNANDO and H. KRONMÜLLER, *Phys. Status Solidi (a)* **125** (1991) 657.

Received 19 April

and accepted 13 November 1996